Noncoplanar $^2H(p,2p)n$ reaction

D. I. Bonbright,* A. M. McDonald,† W. T. H. van Oers, and J. W. Watson‡
Cyclotron Laboratory, Department of Physics, University of Manitoba, Winnipeg, Manitoba R3T 2N2, Canada

H. S. Caplan
Department of Physics, University of Saskatchewan, Saskatoon, Saskatchewan S7N 0W0, Canada

J. M. Cameron, J. G. Rogers,§ and J. Soukup
Nuclear Research Center, University of Alberta, Edmonton, Alberta T6E 2J1, Canada

W. M. Kloet‖
Theoretical Division, Los Alamos Scientific Laboratory, Los Alamos, New Mexico, 87545

C. Stolk¶ and J. A. Tjon
Institute for Theoretical Physics, University of Utrecht, Utrecht, The Netherlands
(Received 7 May 1979)

Calculations based upon the Faddeev equations and measurements of proton-induced deuteron disintegration cross sections have been made at 23.0 and 39.5 MeV for two types of constant-relative-energy loci. In the first configuration the variation of the breakup cross section was studied for fixed values of the final state NN relative energies and a fixed momentum of one of the emerging protons. In the second configuration the variation of the breakup cross section was studied for equal relative energies between all three pairs of nucleons with the two protons emerging with equal momenta symmetrically with respect to the incident beam direction. At 39.5 MeV calculations and measurements were made of both types of loci while at 23.0 MeV only the second kinematical configuration was studied.

[NUCLEAR REACTIONS $^2H(p,2p)n$ at $T_p=23.0$ and 39.5 MeV, measured two types of constant-relative-energy loci; comparisons with three-body calculations using the Reid soft-core potential.]

I. INTRODUCTION

In recent years there have been numerous investigations in the low energy region of systems consisting of three nucleons. These studies included measurements of N-d elastic scattering differential cross sections and vector and tensor analyzing powers, as well as nucleon induced deuteron disintegration in kinematically incomplete and complete experiments. With the evolution of exact three-body calculations based upon the Faddeev equations there has been a continuous interplay between improved theoretical predictions and carefully selected high precision experimental data.[1] Whereas the original Nd theoretical calculations used S-wave local or separable NN potentials, the more recent calculations have used realistic potentials. Benayoun *et al.*[2] reported results for the interaction of Sprung-de Tourreil, type C, with the $^1S_0$, $^3S_1$-$^3D_1$, $^1P_1$, and $^3P_{0,1,2}$ waves treated exactly and the $^1D_2$ and $^3D_2$ waves added perturbatively. Comparison with experimental elastic scattering data at 14 MeV incident nucleon energy showed very good agreement with the exception of the deuteron vector analyzing power. Stolk and Tjon[3] reported on results for the Reid soft-core potential with the tensor part and P waves and D waves treated perturbatively. Although the use of perturbation methods to calculate the spin observables in elastic scattering may need further scrutiny in some cases,[4] agreement with experiment is impressive.

The experiments studying nucleon induced deuteron disintegration have been concerned mainly with regions of phase space where two-body effects prevail as in, e.g., quasifree scattering and final-state interaction processes. For kinematically complete experiments this implies coplanar geometries. As in the case of elastic scattering experiments, the ultimate aim of the deuteron disintegration experiments is a detailed comparison with exact three-body calculations based upon the Faddeev equations. Even relaxing the condition that comparisons should properly be made with predictions calculated using NN potentials which are phase equivalent (i.e., potentials which reproduce equally well the NN on-energy-shell experimental information), the observed differences are not much larger than the experimental uncertainties for most deuteron disintegration data. Consequently, relatively little has been learned from such comparisons.

In order to find a region of phase space where the differences between calculations with different

potential models become really significant, Kloet and Tjon[5] performed a search of four-dimensional phase space mapping the differences of the predictions for two local S-wave NN potentials. It was found that the greatest differences occurred in the regions of cross-section minima where the breakup amplitude for the state with total spin $S=\frac{1}{2}$ and spin for the pair of identical nucleons $S_{NN}=0$ [denoted as $M(\frac{1}{2},0)$] is the only nonzero amplitude. The occurrence of such minima is due to a delicate cancellation of the single-scattering or Born part with the multiple-scattering part or remainder of this breakup amplitude. The value of the cross section in these regions depends in a subtle way on the dynamics of the three-body scattering, as expressed in the Faddeev equations.

In the present study two kinematical configurations were chosen to investigate these interference effects. In the first configuration the variation of the breakup cross section was studied for fixed values of the final-state NN relative energies and a fixed momentum of one of the emerging protons. By choosing, as suggested by Jain, Rogers, and Saylor,[6] particular equal relative energies between the two protons and the neutron one ensures that the cross section is dominated by the $M(\frac{1}{2},0)$ amplitude.

In the second configuration the variation of the breakup cross section was studied along loci which are defined by the requirements of equal values for the final-state NN relative energies and of symmetry with respect to the incident beam direction for the momenta of the two emerging protons. In this kinematical situation only the crucial $M(\frac{1}{2},0)$ doublet amplitude contributes.

Recently, Stolk and Tjon[7] extended their calculations to nucleon induced breakup near 23 and 46 MeV. Whereas there are difficulties in reproducing the vector analyzing powers for the $^2\mathrm{H}(\vec{p},p)np$ and $^1\mathrm{H}(\vec{d},p)np$ reactions at 22.7 MeV incident nucleon energy (possibly related to the convolution of the n-p relative energy in the final-state interaction region), there is considerable improvement over local S-wave type calculations in the agreement with the 23.0 MeV symmetric-constant-relative-energy locus of the present experiment.

In the present paper a detailed comparison is made between experimental results for a particular [Jain, Rogers, and Saylor (JRS)] locus at 39.5 MeV and for the symmetric-constant-relative-energy loci at 23.0 and 39.5 MeV and theoretical predictions of three-body calculations using the Reid soft-core NN potential. The experimental arrangements and procedures are described in Secs. II and III, while data reduction and analysis are described in Sec. IV. Experimental results and the comparison with theoretical predictions are reported in Sec. V. Finally, Sec. VI presents a discussion of the results and some conclusions.

II. EXPERIMENTAL ARRANGEMENTS

The experiment was performed on an external beam line of the University of Manitoba sector-focused cyclotron. The energy of the proton beam was determined by a 45° deflection through a calibrated bending magnet. The calibration of the bending magnet followed from cross-over measurements[8] using thin CH_2 and CD_2 targets at a number of energies in the range 20–50 MeV and by observation of the well-known $J^\pi=\frac{3}{2}^+$ resonance in ^{5}Li at an excitation energy of 16.68 MeV (corresponding to an incident proton energy of 23.39 MeV).[9] From these and previous measurements the calibration of the bending magnet was found to be accurate to ±0.15% in the momentum. The energy spread of the momentum analyzed beam was calculated to be about 200 keV full width at half maximum (FWHM) at 40 MeV for the slit settings used.

The scattering chamber (71 cm internal diameter) contained two counter telescopes, one of which could be moved in a horizontal plane through the incident beam direction, while the second one could be moved to practically any position in the upper hemisphere. A standard gas scattering geometry was adopted. Each counter telescope consisted of a slit with a parallel straight-edged aperture perpendicular to a plane through the direction of the detected particle and the incident beam, an antiscattering baffle, and a solid angle defining collimator with rectangular aperture followed by a set of detectors. The first counter telescope could be set remotely with an angular precision of ±0.05°, while the second "out-of-plane" counter telescope could be set to ±0.2° in α and ±0.5° in β. The notation used, as well as the relation between the angles α and β and the set of spherical coordinates θ_4 and ϕ_4, is indicated in Fig. 1. The accuracy with which the out-of-plane collimator system could be set perpendicular to its scattering plane was $\Delta\epsilon=\pm0.5°$. All collimators were fabricated from nickel (0.28 cm thick) and had straight-edged apertures. Nickel was selected for the collimators because of its low slit edge scattering for a given thickness and its low neutron production cross section.[10] The collimator geometry is given in Table I following the notation of Silverstein.[11] Each detector system consisted of a 200 μm thick surface barrier ΔE detector for timing and particle identification, a 5 mm thick lithium drifted silicon E detector for energy determination of the breakup protons, and a 500 μm thick surface bar-

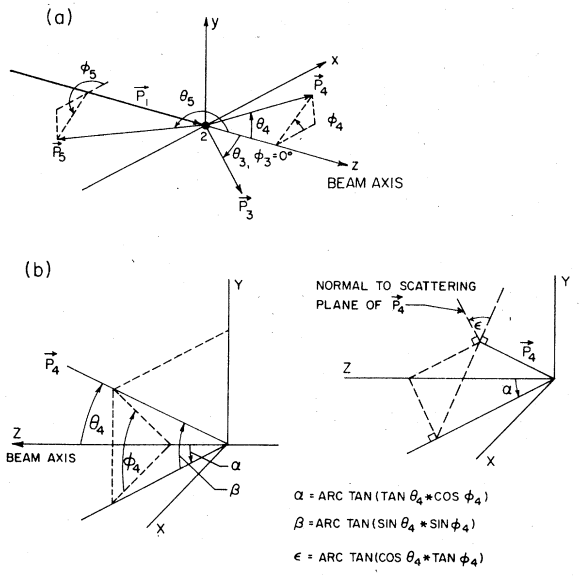

FIG. 1. (a) Angle convention adopted for the three-body breakup reaction $p + d \rightarrow p + p + n$ $(1+2 \rightarrow 3+4+5)$. (b) Relationship between the noncoplanar equipment angular settings $(\alpha, \beta, \epsilon)$ and the spherical coordinates (Θ_4, ϕ_4).

rier VETO detector for rejection of elastically scattered protons. All detectors had sensitive areas of 200 mm^2. The in-plane and out-of-plane detector systems were cooled to −30 °C and −20 °C by a freon refrigeration unit and a Peltier cooler, respectively.

The deuterium gas (99.5% purity) was contained in a hemispherical gas cell which had a window in the horizontal plane through the scattering chamber center 1.90 cm high extending over 360° with the exception of two support posts 20° and 40° wide, and a window in a vertical plane through the scattering chamber center 1.60 cm wide extending over 90°. The gas cell was attached to the noncoplanar equipment. The windows were covered with 25 μm Kapton-H foil. The gas pressure was measured at the beginning and at the end of each experimental run with a precision mechanical absolute pressure gauge calibrated to an accuracy of ±3.5 Torr. Standard data-taking conditions were with pressures ranging between 1250 and 1500 Torr. Monitoring of the gas pressure was possible using closed circuit television. The temperature of the gas was monitored continuously by measuring the resistance of a calibrated thermistor embedded in the inside wall of the gas cell. The temperature was measured to an accuracy of 0.5°. To prevent buildup of contaminants, the gas cell was flushed *in situ* at the beginning of each run with the scattering chamber under vacuum.

The proton beam traversing the scattering chamber was captured in a well shielded, 1.75 m long Faraday cup lined with 2.5 cm thick graphite. The vacuum in the Faraday cup was separated from the vacuum in the scattering chamber by two 50 μm thick Kapton-H foils and 4.0 cm of air. The electrical resistance between the steel casing of the Faraday cup and its central graphite core was 10^{15} ohms. A copper suppressor ring inside the Faraday cup was maintained at −1.5 kV with respect to the steel casing to prevent secondary electrons from entering or leaving the graphite core. The beam current was monitored by a charge integrator with a quoted accuracy of 0.2%. However, due to uncertainty in the charge collection efficiency of the Faraday cup and the existence of beam halo a more realistic uncertainty of 1% was assumed.

The electronic instrumentation consisted of standard fast and slow electronic modules. All detectors were followed by charge-sensitive preamplifiers. Timing information was derived from the ΔE detectors by using fast linear amplifiers, variable band pass timing filter amplifiers, constant fraction pulse height discriminators, and a time-to-amplitude converter (TAC). To reduce radio-frequency (rf) pickup, shorted clipping stubs of length $\frac{3}{2}$ times the wavelength of the rf noise were connected at the input of the band pass filter amplifiers. The noise reduction achieved by this method was a factor of 5. To further reduce

TABLE I. Geometry of the in-plane and out-of-plane collimation systems.

Detector	R (cm)	h (cm)	$2a$ [a] (cm)	1 [a] (cm)	$2b$ (cm)	Ω (10^{-3} sr)	$\Delta\Omega/\Omega$ (%)
In-plane set I	14.73	8.89	0.398	0.596	0.401	1.016	1.6
In-plane set II	14.73	8.89	0.298	0.392	0.297	0.470	2.2
Out-of-plane	14.73	8.89	0.402	0.597	1.598	1.016	1.6

[a] Note that the solid angle defining apertures had rounded-off corners.

electronic noise the detector systems and the scattering chamber were electrically isolated from each other and from their surroundings. Great care was taken not to introduce any ground loops. The time resolution obtained was well within the 35 nsec separating cyclotron beam bursts. Typical values were 8 nsec FWHM or better at 39.5 MeV and 4 nsec FWHM at 23.0 MeV. Pulses from the VETO detectors were passed through shaping amplifiers and fed into timing single channel analyzers, (TSCA's). The output pulses of these TSCA's were fanned in to the inhibit input of the TAC. Pulse height information was extracted from the ΔE and E detectors using shaping amplifiers, delay amplifiers, pulse stretchers, and analog-to-digital converters (ADC's). The output of the TAC generated a master coincidence pulse which opened the ADC linear gates to initiate event processing and also provided a 1.5 μsec wide clock pulse to allow storage of any pileup flags present. Pileup pulses were generated if events in a ΔE branch followed each other within 4 μsec. For each event five linear signals were stored by the PDP15/40 computer: the ΔE pulses, the linear sums of ΔE and E pulses, and the timing signal. The TAC spectrum with pileup pulses removed was monitored continuously during the experimental runs by a 4000 channel pulse height analyzer. This display provided a sensitive check of the condition of the ΔE detectors and of the performance of the ΔE branch of the electronics. In addition, the spectrum of deuterons observed by the in-plane detector and stored in a second pulse height analyzer provided an independent check of the cross section determination by comparison with known p-d elastic scattering differential cross sections.[12]

The data were accumulated in the computer as two 64×64 channel T_3 versus T_4 arrays, one for real plus accidental coincidence events and one for accidental coincidence events over three beam bursts. The data were also recorded event by event on magnetic tape for later off-line analysis. Of the two pulse height analyzer spectra, only the spectrum of deuterons observed by the in-plane detector was recorded for later analysis.

III. EXPERIMENTAL PROCEDURES

A waist of the incident proton beam was positioned at the center of the scattering chamber. After passing the momentum analyzing slits in the focal plane of the 45° bending magnet, no further beam defining collimators were employed. The direction of the incident beam was checked using two NaI monitor counters with closely similar geometries located at 37.5° on either side of the scattering chamber. Observing protons elastically scattered by a 1 mg cm^{-2} thick nickel foil adjustments were made in the beam transport parameters until the two yields agreed to within 1%. It was found that the beam axis did not vary by more than 0.2 degrees over a period of a few days. Typical beam currents were 50 nA on target. The beam spot size was approximately 2 mm wide by 4 mm high with an angular divergence less than 16 mrad.

The angular calibration was checked by moving the out-of-plane counter telescope into the horizontal plane ($\phi_3 - \phi_4 = 180°$) and measuring the angular distribution of p-p coincidences corresponding to p-p elastic scattering. This procedure was followed several times during each series of measurements, giving results consistent with the angular uncertainties quoted above.

The initial energy calibration of the counter telescopes was made with a precision pulser. The final energy calibration and determination of zero offsets were achieved by obsering p-p and p-d coincidence events from hydrogen and deuterium, respectively. Seven angle pairs were selected to provide a calibration from the lowest detectable energy in the counter telescopes to the maximum energy of interest.

Data collection times varied between four hours when both detectors were coplanar to about 30 hours in noncoplanar regions in the neighborhood of the minimum of the cross section.

IV. DATA ANALYSIS AND REDUCTION

Preliminary analysis of the data was done on-line to enable particle identification and to display the energy spectra of coincident pp events. A complete analysis of the data was performed off-line using the recorded events on magnetic tape. The differential cross sections $d^5\sigma/(dT_3 d\Omega_3 d\Omega_4)$ were obtained using the measured gas scattering geometry, the target-gas pressure and temperature, and the Faraday cup integration of the incident beam current. Corrections to the data were made for the effects of dead time and pileup rejection. Typical dead time corrections were from 1% to 3%, while the pileup corrections ranged from 5% to 10%. The gas scattering geometry factor calculated for the in-plane counter telescope was in good agreement with that deduced from the observed yield of recoil deuterons and the known p-d elastic scattering differential cross sections. The cross section error in each channel of the projected energy spectra was deduced from the counting statistics of the "reals" and "randoms" spectra.

The main sources of error contributing to the

TABLE II. Major sources of error contributing to the absolute uncertainty of the cross sections.

Source	Percentage error
Angle setting ($\sin\theta_3$)	≲1.0
Geometry factor in-plane counter telescope	1.9 (set I) 2.8 (set II)
Pressure	~1.0
Temperature	~0.2
Faraday cup integration	≲1.0
Dead time correction	≲0.2
Pileup rejection correction	≲1.0
Veto rejection	≲0.1
Energy of incident proton beam	<1.8

absolute uncertainty in the $^2H(p,2p)n$ disintegration cross sections are summarized in Table II. The systematic errors give an estimated overall normalization uncertainty of ±5% for the projected energy spectra. As the values of the cross sections for the constant-relative-energy loci were determined by fitting a polynomial curve to the data points of the projected energy spectra, a further uncertainty arose. An additional uncertainty of ±5% was possible by varying the number of data points included in the least-squares fit. Summing these errors in quadrature, an overall uncertainty of ±7% in the normalization of the cross sections along the constant-relative-energy loci was estimated.

V. RESULTS AND COMPARISON WITH THEORETICAL PREDICTIONS

A. Locus of Jain, Rogers, and Saylor[13]

In the first kinematical configuration, energy sharing spectra were measured for an incident energy of 39.5 MeV at angle pairs which correspond to seven locations along the JRS locus, defined by $\theta_3 = 27.1°$, $T_3 = 17.87$ MeV, and $T_{35} = T_{45} = 14.37$ MeV. The locus also contains the symmetric coplanar scattering point, i.e., $\theta_3 = \theta_4 = 27.1°$ and $\phi_{34} = 180°$. Figure 2 gives a geometrical representation of the JRS and the symmetric-constant-relative-energy loci. Calculations using the local S-wave NN potential sets MTI-III and MTI-IV of Malfliet and Tjon[14] and the separable YY potential used by Jain and Doolen[15] predicted the existence of a pronounced interference minimum. Of all cases computed the 27.1° JRS locus exhibited the largest difference between the two local S-wave potential predictions at the interference minimum, and this is the reason it was decided to make measurements for this particular locus.

The set of seven energy spectra projected onto the T_3 axis is shown in Fig. 3. The vertical arrow in each energy spectrum at $T_3 = 17.87$ MeV indicates the point at which the above kinematical condition of JRS is satisfied. The data are compared with theoretical predictions for the Reid soft-core potential. The curves labeled $S+T+P+D$ correspond to a two-nucleon T matrix with components due to S-, P-, and D-wave ($^1D_2$ and

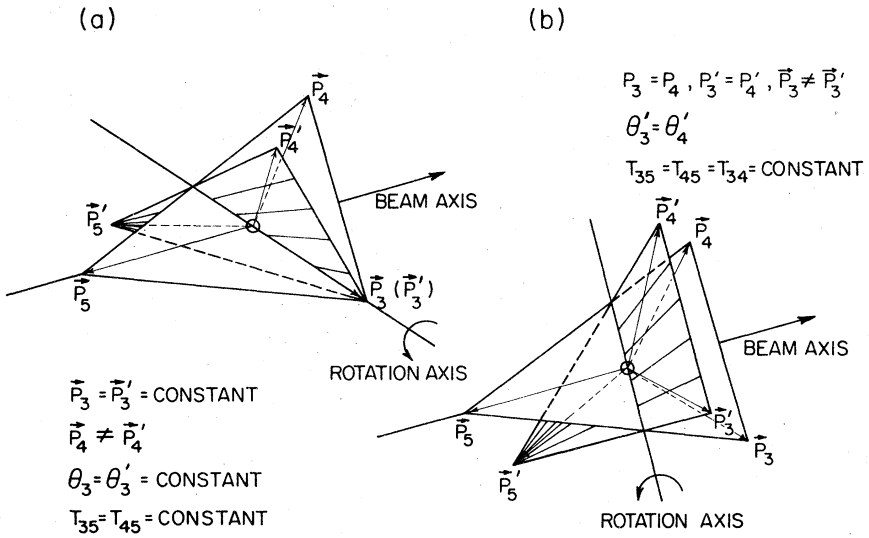

FIG. 2. Momentum triangles of fixed shape in the center-of-mass system. The shaded triangles illustrate the method of rotation chosen: (a) rotation axis recommended by Jain, Rogers, and Saylor (Ref. 6), (b) rotation axis required to preserve the spatial symmetry of nucleons 3 and 4.

$^3D_2$) interactions and the tensor force. The curves labeled S correspond to calculations in which only the S-wave component of the NN interaction is retained, with the deuteron wave function renormalized to unity. One observes that the theoretical predictions for the full Reid soft-core potential reproduce the shape of the energy spectra fairly well. However, there is a tendency of the theoretical predictions to overestimate the magnitude of the cross sections by as much as 20%, which is outside the scale error of the measured differential cross sections. It should be noted that the addition of the higher partial wave components of the NN interaction and the tensor force is constructive except for kinematical configurations close to coplanarity ($\phi_{34} \gtrsim 140°$).

In each spectrum the value of the cross section at $T_3 = 17.87$ MeV was extracted by least-squares fitting a polynomial curve to the data points. The interpolated values are plotted (solid points) as a function of neutron energy T_5 in Fig. 4. The error bars indicate one standard deviation due to the uncertainty in the interpolated value. In addition the interpolated value is somewhat sensitive to the number of data points included in the least-squares fit. As stated above, an additional uncertainty of 5% has been estimated for all interpolated values. It is apparent that the calculations for the full Reid soft-core potential reproduce the energy dependence of the data except for a scale factor. The calculations retaining only the S-wave parts of the potential give an interference minimum which is narrower and deeper than that for the full Reid soft-core potential.

In order to check whether there is appreciable latitude in the behavior of the differential cross section as function of neutron energy within the angular uncertainties, in particular, at the minimum of the cross section, four energy spectra [see Fig. 3(c)] were examined for which the angles

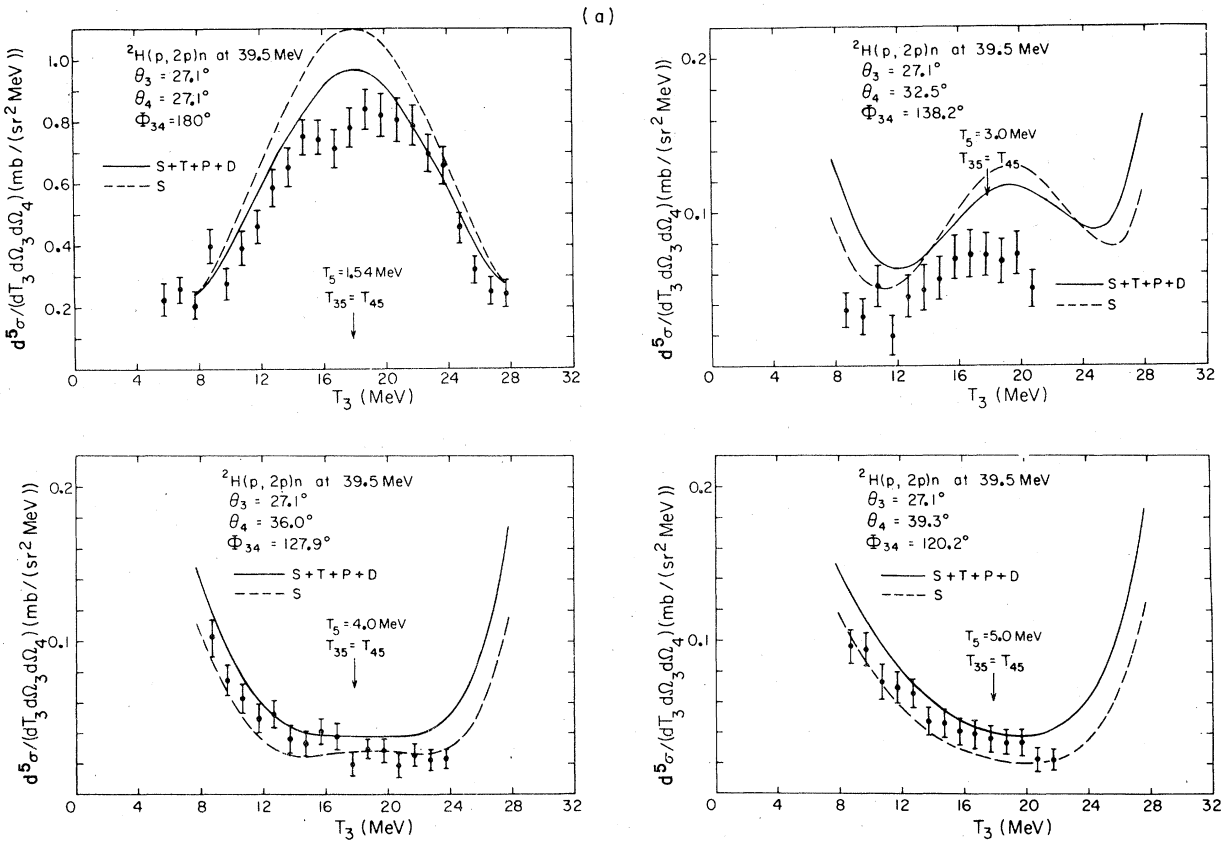

FIG. 3. (a) and (b) Energy spectra for the ^{2}H(p, $2p$)n reaction at 39.5 MeV taken with a fixed nucleon momentum defined by Θ_3 and T_3. The arrows indicate the point at which the relative energy of either proton to the neutron is 14.37 MeV. The curves present theoretical predictions calculated using the Reid soft-core potential. (c) Energy spectra for the ^{2}H(p, $2p$)n reaction at 39.5 MeV taken with a fixed nucleon momentum defined by Θ_3 and T_3. The arrows indicate the point at which the relative energy of either proton to the neutron is close to 14.37 MeV. The curves represent theoretical predictions calculated using the Reid soft-core potential.

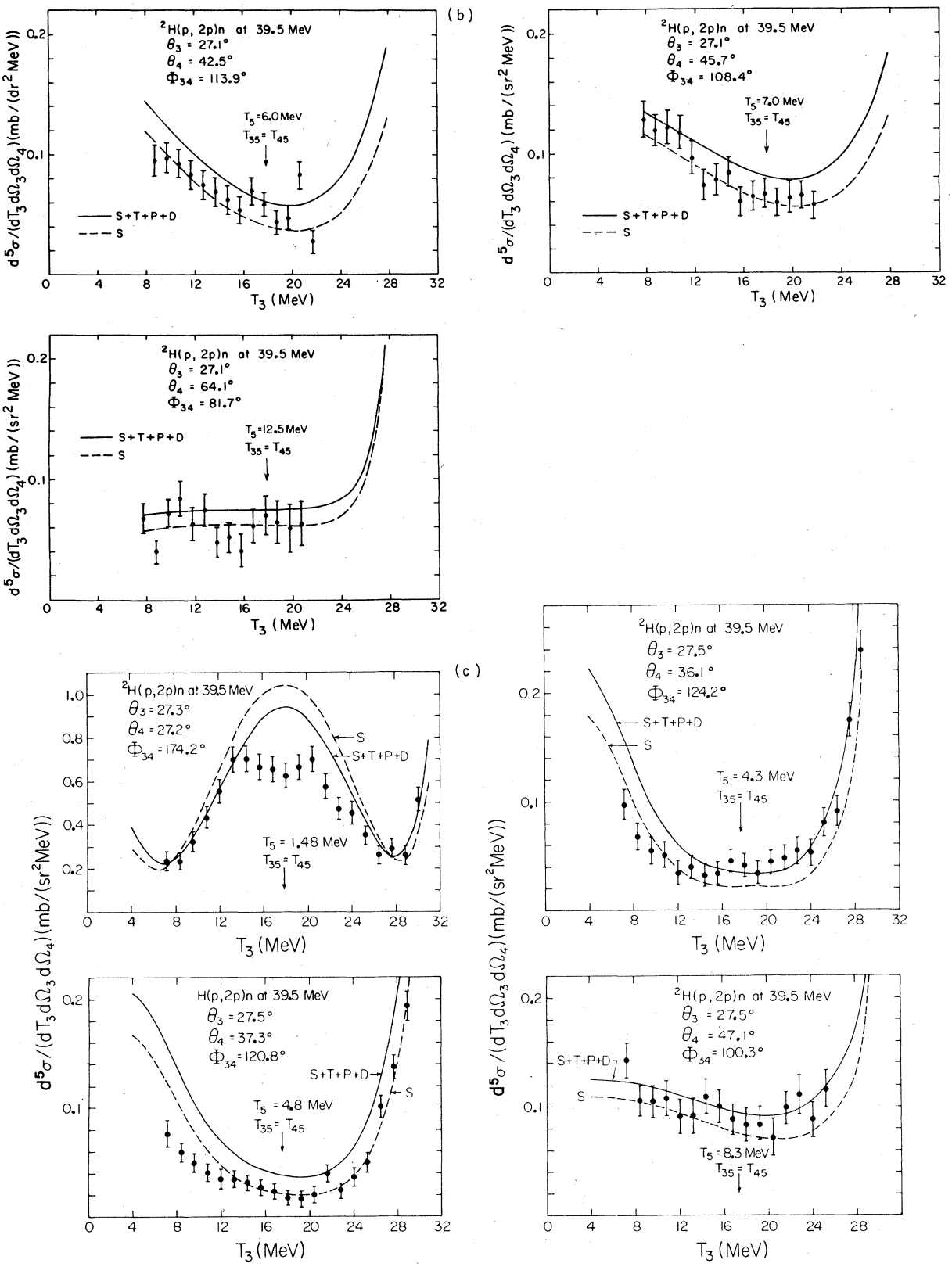

FIG. 3. (*Continued*).

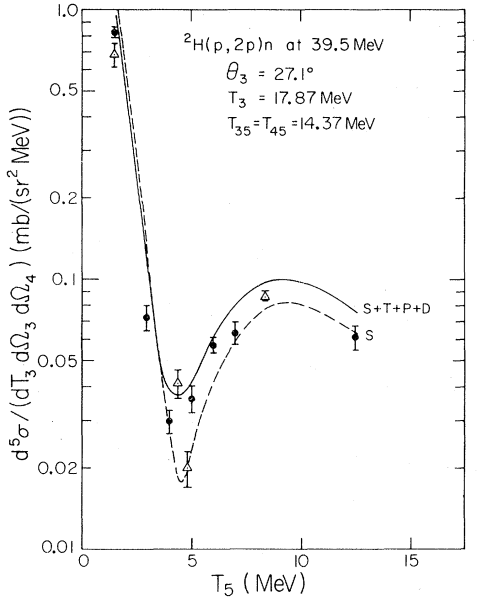

FIG. 4. Data and calculations along a constant-relative-energy locus of Jain, Rogers, and Saylor at 39.5 MeV plotted as a function of the unobserved neutron energy. The difference between the data indicated by solid dots and open triangles is given in the text.

θ_3, α, and β had been set slightly off from the values required. The cross sections deduced from these energy spectra agree within errors with the seven data points extracted from the spectra of Figs. 3(a) and 3(b). The cross sections are shown as the open triangles in Fig. 4. Note that the latter data do not satisfy entirely the kinematical conditions of the particular JRS locus selected ($\theta_3 = 27.1°$, $T_3 = 17.87$ MeV, $T_{35} = T_{45} = 14.37$ MeV).

B. Symmetric-constant-relative-energy loci

Energy spectra were measured in this kinematical configuration at incident energies of 23.0 and 39.5 MeV. The loci have the two protons emerge with equal momenta and at the same polar angles with respect to the incident beam direction. A further condition is that the three nucleon-nucleon relative energies be equal, i.e., $T_{35} = T_{45} = T_{34}$. The lower energy was selected because earlier work[16] indicated good agreement between theory (*S*-wave models) and experimental *n-d* differential elastic as well as total cross sections up to 22 MeV incident energy. It had also been determined that the tensor force, as well as *P*-

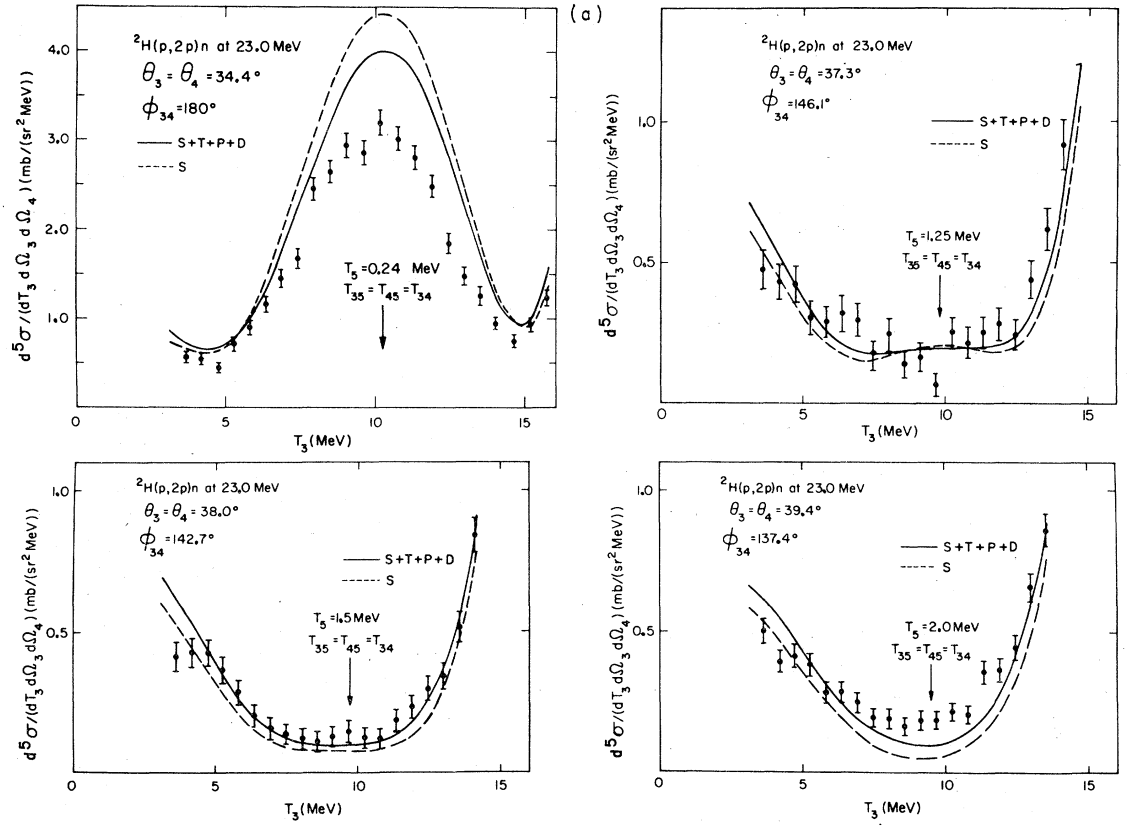

FIG. 5. (a) and (b) Energy spectra for the ^{2}H(p, $2p$)n reaction at 23.0 MeV. The arrows indicate the point at which the three nucleon-nucleon relative energies are equal. The curves represent theoretical predictions calculated using the Reid soft-core potential.

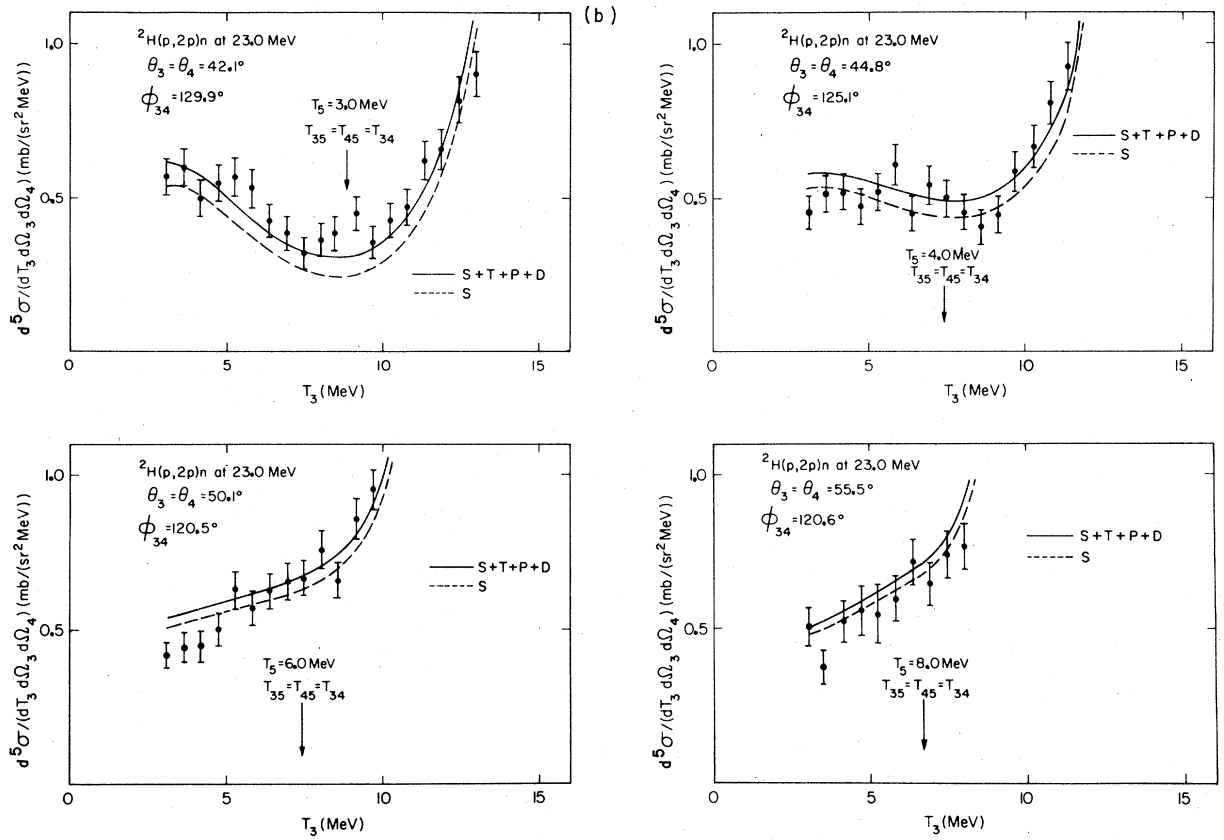

FIG. 5. (*Continued*)

wave interactions, must be included to obtain limited quality fits to the experimental vector and tensor analyzing powers in n-d elastic scattering at 14.1 and 22.7 MeV.[17] More recently, it has been shown that the inclusion of D-wave interactions is essential in order to obtain an improved fit to the vector analyzing powers.[18,3,2] Furthermore, if genuine three-body forces are of importance, one expects to find the greatest sensitivity for loci with equal NN relative energies. Thus it is of great interest to determine the quality of the agreement between Nd breakup data along symmetric-constant-relative-energy loci and theoretical predictions based upon simple NN S-wave and more realistic potential models.

Energy spectra were measured at 23.0 MeV at angle pairs which correspond to eight points on the symmetric-constant-relative-energy locus. The set of eight energy spectra, projected onto the T_3 axis, is shown in Fig. 5. The vertical arrow in each spectrum indicates the point at which the kinematic condition $T_{35} = T_{45} = T_{34}$ is satisfied. The error bars in these spectra give the statistical uncertainty after background subtraction. The reproducibility of the data was checked by repeating the measurement corrresponding to $T_5 = 0.24$ MeV. The two sets of data were taken at the start and end of the 23.0 MeV experiment. After smoothing the data by fitting a polynomial, the difference in magnitude of the cross sections at $T_3 = 10.3$ MeV (i.e., where $T_5 = 0.24$ MeV) is 2.7%, a result well within the accuracy of the data. Differential cross sections were extracted from the eight energy spectra by interpolation after fitting a polynomial curve to the data points of each spectrum. The interpolated values with their errors obtained in this manner are presented in Fig. 6 as function of neutron energy.

The theoretical predictions for the full Reid soft-core potential give an excellent representation of the data with the exception of the energy spectrum measured with coplanar geometry. In particular, the theoretical predictions for the full Reid soft-core potential give the appropriate filling in of the deep interference minimum present when only the S-wave potentials are retained in the calculations (Fig. 6). It has been shown that at 23.0 MeV it is primarily the addition of the P-wave components of the NN interaction which is responsible for filling in this minimum.[7] The contribution of the tensor force is small and that of the other D-wave components of the NN interaction is negligible at

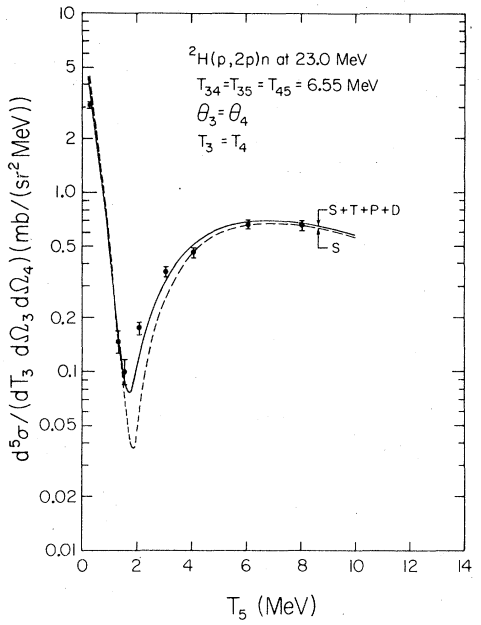

FIG. 6. Data and calculations for the symmetric-constant-relative-energy locus at 23.0 MeV plotted as function of the unobserved neutron energy.

this energy.

Energy spectra measured for eight points on the symmetric-constant-relative-energy locus at 39.5 MeV and projected onto the T_3 axis are shown in Fig. 7. The error bars indicate the statistical accuracy after background subtraction. Also shown are the various theoretical predictions. The breakup cross section as a function of neutron energy T_5 is presented in Fig. 8. In the latter figure the measured value of the cross section at the minimum ($T_5 = 3.0$ MeV) is more than an order of magnitude larger than the theoretical prediction using the S-wave components of the Reid interaction. To check the importance of kinematic broadening, the measurement of two energy spectra was repeated with a smaller set of collimators (set II of Table I) for the in-plane counter telescope. The smaller collimator set gives a reduction by a factor of 2.6 in the gas scattering geometry factor. At $T_5 = 9.0$ MeV the two measurements of the breakup cross section agree within 3.3%, while at $T_5 = 3$ MeV, location of the minimum, the value measured with the smaller colli-

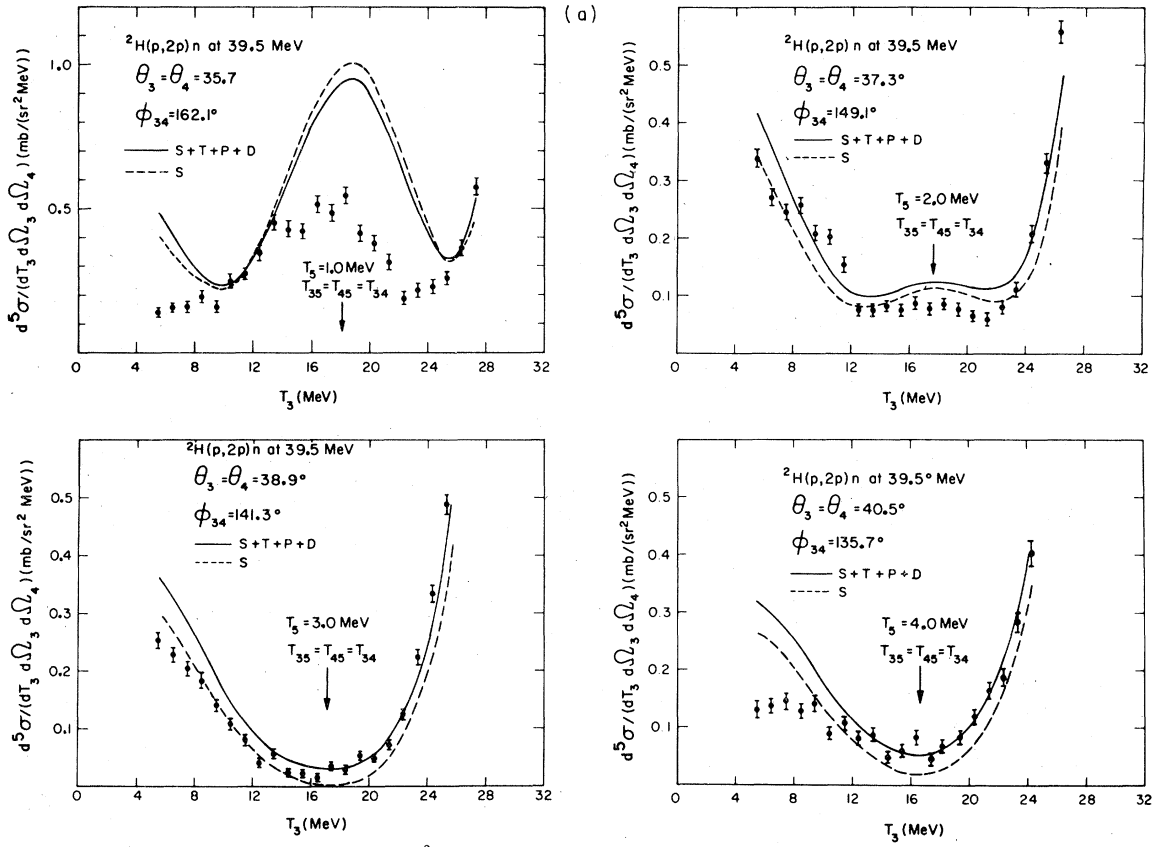

FIG. 7. (a) and (b) Energy spectra for the ^{2}H$(p,2p)n$ reaction at 39.5 MeV. The arrows indicate the point at which the three nucleon-nucleon relative energies are equal. The curves represent theoretical predictions calculated using the Reid soft-core potential.

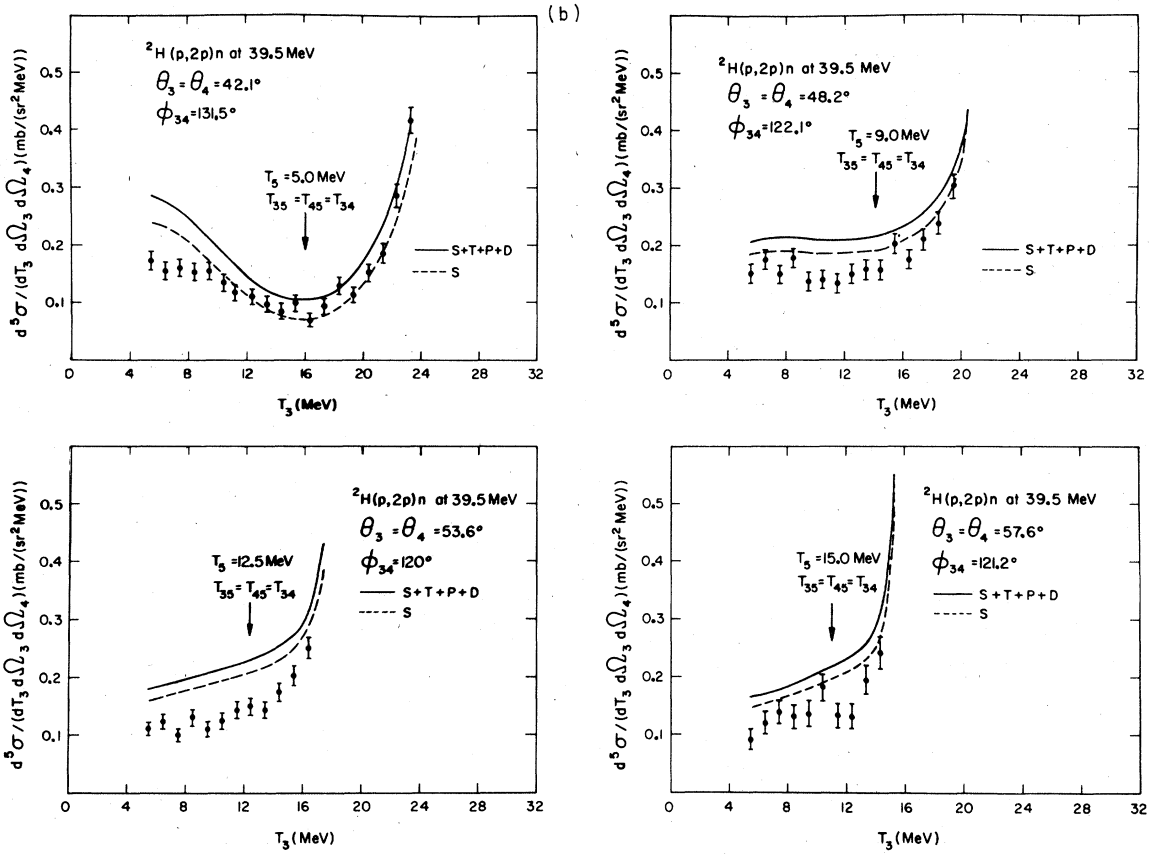

FIG. 7. (*Continued*)

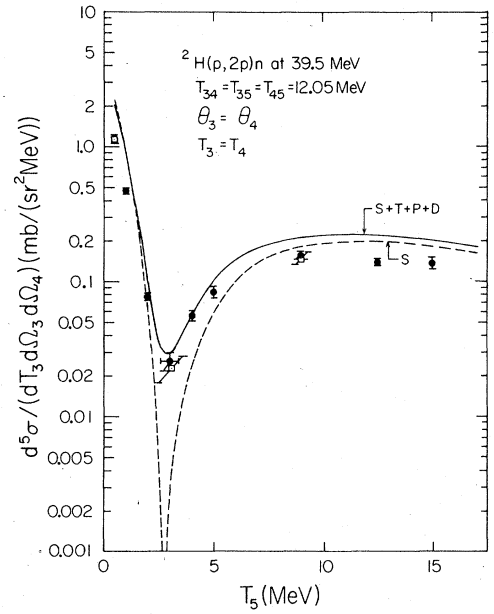

FIG. 8. Data and calculations for the symmetric-constant-relative-energy locus at 39.5 MeV plotted as function of the unobserved neutron energy. The data points presented by open squares were measured with the smaller in-plane collimator set.

mator set, is 9.7% lower than the previous value. One may conclude that the measured value of the cross section at the minimum is not strongly dependent on the finite geometry of the collimation system adopted for the experiment. An additional measurement was made for $T_5 = 0.55$ MeV. The measurements made with the smaller collimator set are shown as open squares in Fig. 8.

As a further check on the effects of finite geometry the maximum possible kinematical spread in the neutron energy T_5 was calculated at the location of the minimum. The calculation took into account the angular widths $\Delta\theta$ and $\Delta\phi$ of both of the rear collimators. The results are indicated by the horizontal error bars in Fig. 8. As shown in Fig. 7 the theoretical predictions based upon the full Reid soft-core potential give a fair representation of the shape of the measured energy spectra. Along the symmetric-constant-relative-energy locus the differences between the theoretical prediction and the data are as large as 30%, which is not inconsistent with that observed for the JRS locus at 39.5 MeV. It should also be noted that when only the S-wave components of the NN interaction are retained, the calculations give a

very deep minimum with a cross section value almost two orders of magnitude smaller than that observed experimentally and than that given by the full Reid soft-core potential calculation. Calculations made for an incident energy of 46.3 MeV showed a quite distinct dependence on the P-wave components of the NN interaction and near the interference minimum also on the tensor force and the D-wave components of the NN interaction.[19] The only other study of the noncoplanar $^2\mathrm{H}(p, 2p)n$ reaction under kinematical conditions chosen away from the dominance of two-body scattering processes was made at an incident energy of 44.9 MeV.[20] Theoretical predictions with the full Reid soft-core potential calculated for an incident energy of 46.3 MeV give the same qualitative agreement with these data.[19] Numerical values of the differential cross section data can be obtained as an addendum to this paper from the authors.

VI. DISCUSSION AND CONCLUSIONS

Coulomb effects have been ignored in the calculations. Only very recently has a framework been constructed that allows inclusion of the long range Coulomb force in an exact way.[21] Ebenhöh *et al.*[22] have shown that Coulomb effects are important in the p-d breakup reaction at an incident proton energy of 10 MeV. But for relative energies above 10 MeV Coulomb effects are negligible and decrease with increasing p-p scattering angles. For example, at 90° in the center of mass, Coulomb effects are not important for energies above 3 MeV, and thus would not appreciably effect the single-scattering term. In the multiple-scattering term the p-p scattering angles and relative energies can take on all values between zero and the maximum kinematically possible. Consequently, Coulomb effects are expected to modify this term, which is important at large values of T_3, the energy of the unobserved neutron.[23] The quality of the agreement between the calculations with the full Reid soft-core potential and the experimental data at 23.0 MeV indicates that Coulomb effects play a minor role. Therefore, the difference between theory and experiment at 39.5 MeV for large values of T_5 must be accounted for by more intricate aspects of the calculations, such as the use of perturbative methods and the neglect of higher partial wave components of the NN interaction. Only after these aspects of the calculations have been assessed thoroughly may one infer that differences between theory and experiment are the result of a different behavior of the off-energy-shell interactions and/or genuine three-body forces.

For geometrical configurations close to coplanarity, the theoretical curves need to be normalized by a factor of 0.6–0.8 to obtain agreement with the experimental data. Here the theoretical predictions for the full Reid soft-core potential and for only the S-wave components of the Reid potential differ by at most 15%, the S-wave potential model predictions being the larger. It was noticed that for the S-wave potential model calculation, the term corresponding to interference between single- and multiple-scattering parts of the amplitude is very important in reducing the magnitude of the cross section predictions in the region of coplanarity.[23]

The inclusion of the tensor force and of the P- and D-wave components of the NN interaction appears to give about the right filling in of the interference minima for all three loci. Chiefly, the P-wave components are responsible for filling in the minimum at 23.0 MeV, but at 39.5 MeV the D-wave components and the tensor force are also important.

There lies an intrinsic difficulty in separating out the effects due to the off-energy-shell behavior of the two-body T matrices and those due to three-body forces. Both effects should be maximum when all three nucleons are close to each other. This requires the two like nucleons to be in a spin singlet state, a condition which is met by the present experiment. The breakup amplitude $M(\frac{1}{2}, 0)$ is the only nonzero amplitude for the symmetric-constant-relative-energy loci. The kinematical configuration most likely to display sensitivity to possible three-body forces is characterized by equal laboratory energies for all three nucleons in addition to equal relative energies between the nucleon pairs. At an incident energy of 23.0 MeV this kinematical condition corresponds to $T_5 = 6.9$ MeV. At this energy no deviations from the two-body potential model calculations are observed. At 39.5 MeV the data at $T_3 = T_4 = T_5 = 12.4$ MeV are approximately 0.65 times the theoretical predictions. However, due to the overall discrepancies between data and theory at this incident energy, no definite conclusions can be drawn concerning possible three-body forces.

This work was supported in part by the AECB and NRC of Canada.

*Present address: Data/Ware Development, Inc., San Diego, California 92121.
†Present address: Power Projects of Atomic Energy of Canada, Ltd., Mississauga, Ontario, L5K 1B2.
‡Present address: Department of Physics, Kent State University, Kent, Ohio 44242.
§Present address: TRIUMF, Vancouver, B. C., Canada, V6T 1W5.
‖Present address: Department of Physics, Rutgers University, New Brunswick, New Jersey 08873.
¶Present address: Gemeentelyk Bureau voor Onderzoek en Statistiek, Rotterdam, The Netherlands.

[1]See for instance G. G. Ohlsen, *Few Body Systems and Nuclear Forces II*, edited by H. Zingl, M. Haftel, and H. Zankel (Springer, Berlin, 1979), p. 295.
[2]J. J. Benayoun, J. Chauvin, C. Gignoux, and A. Laverne, Phys. Rev. Lett. 36, 1438 (1976).
[3]C.Stolk and J. A. Tjon, Phys. Rev. Lett. 35, 985 (1975).
[4]W. M. Kloet, in *Nucleon-Nucleon Interactions—1977*, proceedings of the Second International Conference on Nucleon-Nucleon Interaction, edited by D. F. Measday, H. W. Fearing, and A. Strathdee, AIP Conference Proceedings No. 41, New York, 1978), p. 392.
[5]W. M. Kloet and J. A. Tjon, Nucl. Phys. A210, 380 (1973).
[6]M. Jain, J. G. Rogers, and D. P. Saylor, Phys. Rev. Lett. 31, 838 (1973).
[7]C. Stolk and J. A. Tjon, Phys. Rev. Lett. 39, 395 (1977).
[8]B. M. Bardin and M. E. Rickey, Rev. Sci. Instrum. 35, 902 (1964); R. Smythe, *ibid.* 35, 1197 (1964).
[9]P. Darriulat, D. Garreta, A. Tarrats, and J. Testoni, Nucl. Phys. A108, 316 (1968); S. N. Bunker, J. M. Cameron, M. B. Epstein, G. Paic, J. R. Richardson, J. G. Rogers, P. Tomaš, and J. W. Verba, *ibid.* A133, 537 (1969).
[10]E. J. Burge and D. A. Smith, Rev. Sci. Instrum. 33, 1371 (1962); F. G. Resmini, A. D. Bacher, D. J. Clark, E. A. McClatchie, and R. de Swiniarski, Nucl. Instrum. 74, 261 (1969).
[11]E. A. Silverstein, Nucl. Instrum. 4, 53 (1959).
[12]S. N. Bunker, J. M. Cameron, R. F. Carlson, J. R. Richardson, P. Tomaš, W. T. H. van Oers, and J. W. Verba, Nucl. Phys. A113, 461 (1968).
[13]For a preliminary account of these results see A. M. McDonald, D. I. Bonbright, W. T. H. van Oers, J. W. Watson, J. G. Rogers, J. M. Cameron, J. Soukup, W. M. Kloet, and J. A. Tjon, Phys. Rev. Lett. 34, 488 (1975).
[14]R. A. Malfliet and J. A. Tjon, Nucl. Phys. A127, 161 (1969).
[15]M. Jain and G. D. Doolen, Phys. Rev. C 8, 124 (1973).
[16]W. M. Kloet and J. A. Tjon, Ann. Phys. (N. Y.) 79, 407 (1973).
[17]J. C. Aarons and I. H. Sloan, Nucl. Phys. A182, 369 (1972); S. C. Pieper, *ibid.* A193, 529 (1972); Phys. Rev. C 6, 1157 (1972); 8, 1702 (1973).
[18]P. Doleschall, Nucl. Phys. A220, 491 (1974).
[19]C. Stolk and J. A. Tjon, Nucl. Phys. (to be published).
[20]D. L. Shannon, W. Breunlich, I. Slaus, J. W. Sunier, G. A. Anzelon, E. S. Y. Tin, W. T. H. van Oers, M. B. Epstein, and W. Ebenhöh, Nucl. Phys. A218, 381 (1974).
[21]E. O. Alt, W. Sandhas, H. Zankel, and H. Ziegelman, Phys. Rev. Lett. 37, 1537 (1976).
[22]W. Ebenhöh, B. Sundqvist, A. Johansson, L. Amtén, L. Gläntz, L. Gönczi, and I. Koersner, Phys. Lett. 49B, 137 (1974).
[23]A. M. McDonald, Ph.D. thesis, University of Manitoba, 1976 (unpublished).